



Long-term spatiotemporal variations and expansion of low-oxygen conditions in the Pearl River estuary: A study synthesizing observations during 1976-2017

Jiatang Hu^{1,2,3,*}, Zhongren Zhang¹, Bin Wang⁴, Jia Huang⁵

5

¹ School of Environmental Science and Engineering, Sun Yat-sen University, Guangzhou, 510275, China

² Guangdong Provincial Key Laboratory of Environmental Pollution Control and Remediation Technology, Guangzhou, 510275, China

³ Southern Marine Science and Engineering Guangdong Laboratory (Zhuhai), Zhuhai, 519000, China

10 ⁴ Department of Oceanography, Dalhousie University, Halifax, Nova Scotia B3H 4R2, Canada

⁵ Zhongshan Research Institute of Environmental Protection Science Corporation Limited, Zhongshan, 528400, China

Correspondence to: Jiatang Hu (hujtang@mail.sysu.edu.cn)

15 **Abstract.** The Pearl River estuary (PRE) frequently experiences low-oxygen conditions in summer, with large extents of low-oxygen events and a long-term deoxygenation trend being reported recently. In this study, we provide a synthesis of the spatiotemporal patterns and incidence of different low-oxygen levels in the PRE based on the in-situ observations collected from 1976 to 2017, and aim to elucidate the underlying mechanisms of low-oxygen conditions and their changes over the past 4 decades. The long-term observations show that the oxygen content in the PRE had
20 significant temporal variability and spatial heterogeneity. Low-oxygen conditions occurred mostly in the bottom waters of 5-30 meters during summer and early autumn, with locations and severity varying substantially among years. Coastal waters from the southwest of Lantau Island to the northeast of Wanshan Islands were identified as the hotspot area prone to subsurface low-oxygen conditions due to the combined effects of comparatively deep topography, proper residence time and stability of the water column, and enhanced oxygen depletion related to high phytoplankton
25 biomass. In addition, the low-oxygen waters, either directly imported from the upstream reaches or generated locally and further transported with the estuarine circulation, also had considerable impacts on the oxygen levels in the estuary. As for early autumn, marked low-oxygen conditions were present both in the surface and bottom waters. A large area affected by low oxygen (~4,450 km²) was found in September 2006, where the low-oxygen conditions were comparable to the most severe ones observed in summer and formed by distinct mechanisms. Our analysis also reveals
30 an apparent expansion of the summertime low-oxygen conditions at the bottom of the PRE since the years around 2000, coincident with the major environment changes in the Pearl River region. Overall, the PRE seems to be undergoing a



transition from a system characterized by episodic, small-scale hypoxic events to a system with seasonal, estuary-wide hypoxic conditions. Although exacerbated eutrophication associated with anthropogenic nutrient inputs was generally considered the primary cause for the deterioration of low-oxygen conditions in the PRE, the sharp decline in sediment load may play an important role as well via increasing water transparency and thereby supporting higher and broader phytoplankton biomass in the estuary.

Keywords: Dissolved oxygen; Hypoxia; Temporal and spatial variability; Long-term deoxygenation trend; Pearl River estuary

1. Introduction

Oxygen is fundamental to biogeochemical processes and life in aquatic environments. Its decline can impose significant impacts on the aquatic ecosystems. When dissolved oxygen (DO) level drops below 2 mg/L, hypoxic conditions emerge and could have a series of undesirable biological and ecological consequences, such as causing extensive mortalities of fish and dramatic changes in the biological community structures and sediment biogeochemical cycles, promoting the release of greenhouse gases, and aggravating the ocean acidification (Zhang et al., 2010; Cai et al., 2011; Middelburg and Levin, 2009; Diaz and Rosenberg, 2008). In recent decades, hypoxia has frequently occurred in estuaries and coastal waters, largely ascribed to the influence of human activities in combination with global changes (Breitburg et al., 2018; Rabalais et al., 2010). Large-scale hypoxic zones have been observed in a variety of coastal systems, including the Baltic Sea, the northern Gulf of Mexico, Chesapeake Bay, Long Island Sound, and the Yangtze River estuary, with substantial increases in the spatial extent, intensity, and duration of hypoxia in recent years (Fennel and Testa, 2019 and references therein).

A great number of studies have been carried out to investigate the short- and long-term changes, underlying processes, and controlling factors of coastal hypoxia. It was clearly shown that the generation and development of hypoxia in densely populated and urbanized estuaries and other coastal systems are closely linked to the intensifying eutrophication induced by anthropogenic nutrient inputs (Rabalais et al., 2010; Fennel and Testa, 2019). For example, the northern Gulf of Mexico experiences large-scale, persistent hypoxia in the bottom water every summer (with an area of 15,000 km² on average) largely due to the high primary production stimulated by excessive nutrient loads from rivers together with strong density stratification (Bianchi et al., 2010; Rabalais et al., 2002). In addition, physical conditions such as winds and upwelling also play a significant role in regulating the intensity and duration of hypoxia (Yu et al., 2015; Feng et al., 2014). Compared with the northern Gulf of Mexico, the summertime hypoxic zone off the Yangtze River estuary has both common (i.e. the intense stratification and eutrophication-driven primary production are the key mechanisms controlling hypoxia) and unique features. Its formation and evolution are influenced by a more



65 complex interaction of various water masses, including the Yangtze River diluted water, Taiwan warm currents, Kuroshio subsurface water, and upwelled water (Zhang et al., 2018; Wei et al., 2017). Overall, the dynamics of hypoxia in estuaries and coastal waters are controlled by a combination of physical, biological, and chemical processes (e.g., photosynthesis, nitrification, water-column microbial respiration, sediment oxygen uptake), but the predominant ones vary by systems. Also, the susceptibility to developing hypoxic conditions is significantly different among coastal systems, depending on their respective pressures from local pollution loads and capacities to resist such pressures under regional physical and biogeochemical regimes.

70 Located in the south of China, the Pearl River estuary (PRE; Figure 1) is the central area of the Guangdong-Hong Kong-Macao Greater Bay Area, surrounded by several megacities (including Guangzhou, Shenzhen, and Hong Kong). With the rapidly growing population and socioeconomic development, the PRE receives large inputs of nutrients and diverse contaminants, which has led to a wide range of severe problems in the estuary, such as eutrophication, red tides, hypoxia, and decline of fishery resources (Dai et al., 2008; Harrison et al., 2008; Li et al., 2020). There has been a
75 great concern on hypoxia in the PRE since the 1980s. Based on historical observations, Lin et al. (2001) reported for the first time the incidence of bottom-water hypoxia in the PRE. In the follow-up field surveys, hypoxic events were also observed in the western shoal of the Lingdingyang Bay, the outer Modaomen and Huangmaohai Bays, and the waters adjacent to Lantau Island and Wanshan Islands (Su et al., 2017; Cui et al., 2019; Shi et al., 2019; Yin et al., 2004; Lu et al., 2018; Qian et al., 2018; Li et al., 2018; Ye et al., 2013). Extensive research has been conducted to
80 explore the distribution and influential factors of hypoxia in the PRE by means of field observations and numerical simulations. Results showed that hypoxia mainly appeared in the bottom waters during summer, and the freshwater-induced stratification and sediment oxygen consumption are the dominant factors leading to its generation (Zhang and Li, 2010; Wang et al., 2017; Yin et al., 2004); however, due to the combined effects of relatively shallow depth, high water turbidity, strong physical processes, and short duration of vertical stratification (eroded by periodic tidal forcing and strong wind events; Luo et al., 2009; Lu et al., 2018), hypoxia was generally confined to a very small scale and
85 occurred in an episodic and intermittent manner (Li et al., 2020; Rabouille et al., 2008). Nevertheless, notable low-oxygen events, with spatial extents much larger than previous ones, have been reported in recent works (Shi et al., 2019; Lu et al., 2018; Su et al., 2017; Li et al., 2018). Su et al. (2017) reported that the areal extent of bottom $DO < 2$ mg/L in July 2014 exceeded 290 km², and Li et al. (2018) reported that the extent of bottom $DO < 4$ mg/L in June
90 2015 was estimated ~1,500 km². There seems to be a growth of the areas affected by low-oxygen conditions in the PRE. Collectively, the problem of hypoxia has received great attention, but there is still a lack of in-depth investigation on the temporal and spatial variability of DO in the PRE, and the scope, frequency, and intensity of hypoxia as well as its long-term changes are poorly understood. Besides, most of the previous studies focused on the summertime hypoxia, while it is unclear whether hypoxia also exists in other periods. This is an important issue that has long been ignored.



95 In fact, as we will point it out in this study, there was a large area of hypoxia occurring in early autumn as well, which appears to have different features and driving mechanisms from those typically observed in summer.

Here we synthesize the observational data at sites collected during 1976-2017 to explore the temporal and spatial characteristics of DO and the long-term status of low-oxygen conditions in the PRE. Specifically, we investigate the locations, areal extents, and frequencies of occurrence of DO below 2, 3, 4 mg/L, referred to as hypoxia, oxygen
100 deficiency, low oxygen, respectively. We also aim to clarify the key factors controlling low-oxygen conditions and their expansions over recent years.

2. Materials and methods

The data used for analysis comprises multiyear cruise observations in the PRE and its adjacent coastal waters compiled from five datasets (see Table 1 for details). The first dataset includes vertical profiles of salinity, temperature, DO,
105 nutrients (ammonia, nitrate, and phosphate), and suspended sediment concentrations in the water column collected by the South China Sea Environmental Monitoring Center during 1976-2006 (with 42 cruises in total); data on chlorophyll *a* was also available in September 2006. The second dataset contains historical measurements of water quality parameters (including salinity, temperature, DO, nutrients, suspended sediments, and chlorophyll *a*) collected from a summer cruise carried out by the Pearl River Estuary Pollution Project in July 1999 (Chen et al., 2004). The
110 third dataset includes the observed salinity, temperature, and DO profiles collected by the State Oceanic Administration of China from the cruises in four different seasons during 2006-2007. The fourth dataset contains the water quality data (listed in Table 1) collected by the Marine and Fishery Environmental Monitoring Center of Guangdong Province from four seasonal cruises during 2013-2014. The last dataset is comprised of recent observations on bottom-water DO obtained from literature sources, including data in July 2014 (Su et al., 2017), July
115 2015 (Lu et al., 2018), and July 2017 (Shi et al., 2019).

In addition, the DO saturation state (DO_s , in unit of %), calculated as the ratio of the measured DO concentration to its saturation concentration, was also used to assess the severity of oxygen deficits in the PRE. The DO saturation concentration (DO_{sat}) is a function of both salinity and temperature and is computed via the following equation (Hyer et al., 1971):

$$120 \quad DO_{sat} = 14.6244 - 0.367134 \cdot T + 0.0044972 \cdot T^2 + S \cdot (-0.0966 + 0.00205 \cdot T + 0.0002739 \cdot S) \quad (1)$$

where T is temperature ($^{\circ}C$); S is salinity (PSU).



3. Results

3.1 Seasonal variations of DO-related variables in the PRE

Figure 2 shows the spatial means and standard deviations of DO concentrations, DO_s, salinity, and temperature at the surface and bottom of the PRE during different seasons. It can be clearly seen that all these variables had significant seasonal variations. In spring and winter, the average DO concentration was maintained at about 6-9 mg/L (Figure 2a1). The DO level at the bottom was slightly lower than that at the surface. No low-oxygen water with DO < 4 mg/L was found except in May 2014. In spring, the surface salinity primarily varied between 20 and 27 PSU, and the bottom salinity was approximately 2 PSU higher (Figure 2a3). In winter, salinity was high, with very small difference between the surface and bottom, indicating that the water column was well mixed; the average water temperature (17-21 °C) was lower than that in spring overall (Figure 2a4). DO_s in these two seasons were similar, mostly at near-saturation (90%-105%; Figure 2a2).

In summer, the DO content was lower than those in spring and winter, especially in the bottom water (with averages of 3.8-5.8 mg/L; Figure 2b1). Low oxygen (DO < 4 mg/L) was observed in all 19 summer months except August 1976, and oxygen deficiency (DO < 3 mg/L) was observed in 14 out of 19 summer months including July 1987, July of 1991-1992 and 1994-1997, July-August 1999, July 2005, July-August 2006, August 2009, and August 2013. Hypoxia (DO < 2 mg/L) occurred in July of 1987 and 2005. Actually, the DO levels in July of 1997 and 1999 were very close to hypoxic conditions as well, with the minimum concentrations of 2.1 mg/L. Water temperature in summer was comparatively high, with 27.0-30.5 °C at the surface and mostly 24.5-28.5 °C at the bottom (Figure 2b4). Besides, the differences of temperature and salinity between the surface and bottom were evident, especially for salinity (Figure 2b3), showing the presence of pronounced vertical stratification across the water column. Most of the surface DO_s was maintained at 88%-105% (Figure 2b2), but the bottom DO_s was significantly lower (52%-82%).

In autumn, water temperature has decreased compared with summer, but was higher than those in spring and winter, as shown in Figure 2c4. As for salinity, it was close to that in spring. Low-oxygen water was absent in mid-to-late autumn (October and November), when the average DO and DO_s were generally maintained at 6.0-7.5 mg/L and 75%-102% (Figure 2c1-c2), respectively, with small vertical differences. However, in early autumn (September) low oxygen appeared both in the surface and bottom waters, with fairly low DO values (as low as 1.1 mg/L at the surface and 0.8 mg/L at the bottom in September 2006). This reveals the existence of hypoxic events in periods other than summer.

To further explore the spatial characteristics of DO in the PRE, Figures 3 and 4 present the DO distributions at the surface and bottom in different seasons of three decades. As shown, the surface DO in March was high overall and homogenous in space (Figure 3a1), but in April and May, the spatial difference became relatively large (Figure 3b1



and c1). The surface water with $DO < 5$ mg/L appeared near the eastern four river outlets (see Figure 1 for their locations) in April 2007 and May 2014 (with DO as low as 3.5 mg/L). With respect to summer, the surface DO at the open sea was higher than that inside the estuary and often had high values, for example, in the coastal water surrounding Wanshan Islands (Figure 3b2 and c2); low oxygen was observed in the inner Lingdingyang Bay. As for autumn, the surface DO showed a northwest-southeast distribution pattern in October (Figure 3a3 and b3), relatively high on the western side of the PRE, and it exhibited a northwest-southeast pattern in November (Figure 3c3). Compared with other seasons, the surface DO in winter was higher, mostly exceeding 7 mg/L, and it was more uniformly distributed over the PRE (Figure 3b4 and c4).

Regarding the bottom DO, its distribution pattern in March closely resembled the surface one, showing small spatial difference as well (Figure 4a1). Since then, the DO content became progressively lower from April to May (Figure 4b1 and c1), and low oxygen appeared near the eastern river outlets, similar to that at the surface. In summer, the bottom water was frequently subject to apparent low-oxygen conditions. As shown in Figure 4a2, there was a low-oxygen zone extending from the west of Lantau Island to Wanshan Islands in July 1997, and the observed areas of low oxygen (HA_4) and oxygen deficiency (HA_3) were estimated 704 km² and 157 km², respectively. In July-August 2006, a relatively large areal extent of low oxygen was observed, distributed in patchy waters (Figure 4b2); the HA_4 in total reached 955 km². In autumn, the bottom water was re-oxygenated and reinstated to relatively high DO levels (Figure 4a3-c3), displaying spatial patterns analogous to those at the surface. It is also noted that the phenomenon of $DO < 5$ mg/L was observed in the bottom water adjacent to the eastern river outlets in November 2013 (Figure 4c3) as well as in February 2014 (Figure 4c4).

3.2 Long-term changes and hotspot areas of low-oxygen conditions in the summer of the PRE

In order to gain a thorough insight into the interannual and long-term changes of the summertime low-oxygen conditions, Figures 5 and 6 present the DO distributions at the surface and bottom of the PRE in the summer months during 1976-2017 (of which 1997, 2006 and 2013 have been shown earlier and will not be repeated here). In the surface water, the average DO content varied between 5.7 mg/L and 8.3 mg/L, and high DO values (> 8.0 mg/L) were often observed at the open sea (Figure 5). It is interesting to note that the lowest DO observed at the surface before 1999 was 4.8 mg/L (Figure 2b1), which is well above the threshold of low oxygen, but since 1999, low-oxygen water with $DO < 4$ mg/L frequently appeared in the inner Lingdingyang Bay; for example, surface DO levels as low as 3.0 mg/L and 2.8 mg/L were observed in July 2005 (Figure 5c3) and August 2013 (Figure 3c2), respectively. This emerging exacerbation of low-oxygen conditions in the surface water was primarily attributed to the influence of low-oxygen inflows from the upstream reaches and increasing sewage discharge brought by rapid economic development and urbanization in the Pearl River Delta over the past 30 years (Li et al., 2020).



At the bottom, apparent low-oxygen conditions prevailed in all the summer months except August 1976 (a period
185 prior to the implementation of China's reform and opening-up policy), and their locations and spatial extents varied
substantially among different periods (Figure 6). Overall, a majority of the low-oxygen events congregated at the
bottom of 5-30-m isobaths and were present in the vicinity of Humen, at the near-shore of the east of the inner
Lingdingyang Bay (including Shenzhen Bay), along the deep navigation channel (extending from the north of
Neilingding Island to the southwest of Lantau Island), in the shallow water (between 5-10-m isobaths) on the western
190 side of the middle Lingdingyang Bay, at the outer Modaomen-Jitimen-Huangmaohai Bays, and in the waters from the
south of Lantau Island to Wanshan Islands (Figure 7a1-a2). On top of this, the coastal area in the lower estuary,
extending from the southwest of Lantau Island to the northeast of Wanshan Islands, was the hotspot with high
incidence of bottom low-oxygen events, followed by the shallow area east of Hengqin Island (Figure 7b1-b2).

In terms of the spatial extents, low-oxygen conditions in the 1980s and 1990s were restricted within a very small
195 scale, with all the HA_4 and HA_3 estimated smaller than 760 km^2 and 160 km^2 , respectively (Figure 6). The areal
extents of low-oxygen conditions were relatively large in July of 1987 (Figure 6a3), 1994-1995 (Figure 6c2-c3) and
1997 (Figure 4a2). However, since the 2000s, the area affected by low-oxygen conditions has increased, with the HA_4
> $1,600 \text{ km}^2$ being frequently reported. For instance, a more fully developed low-oxygen zone was generated in July
1999 (Figure 6d1). Its central area covered the entire waters of the middle part of the PRE. The HA_4 and HA_3 were
200 estimated $1,602 \text{ km}^2$ and 263 km^2 , respectively. As for July 2005, the HA_4 and HA_3 reached $2,683 \text{ km}^2$ and 304 km^2 ,
respectively (Figure 6d3). A majority of the bottom water resided in low-oxygen conditions, and hypoxia ($\sim 6 \text{ km}^2$)
occurred at the near-shore of the inner Lingdingyang Bay. In particular, recent field investigations during 2014-2017
further indicate the occurrence of large-scale low-oxygen events in the PRE (Figure 6e1-e4). The HA_2 observed in the
205 bottom waters surrounding Lantau Island and Wanshan Islands on July 13-16, 2014 (Leg 1) reached 338 km^2 , with the
minimum DO of 0.9 mg/L , and the HA_4 and HA_3 were estimated $1,290 \text{ km}^2$ and $1,037 \text{ km}^2$, respectively. Subsequently,
a hypoxic zone in similar size was found on July 19-27 (Leg 2) as well, primarily located in the offshore water south of
Wanshan Islands where DO dropped to 0.2 mg/L . The HA_4 and HA_3 reached $3,101 \text{ km}^2$ and $1,123 \text{ km}^2$, respectively.
In July 2015, the low-oxygen zone observed was even larger (reaching $4,453 \text{ km}^2$), but the hypoxic area was relatively
small ($\sim 51 \text{ km}^2$; Figure 6e3). With respect to July 2017, a large area affected by low oxygen was observed, with the
210 HA_4 , HA_3 , and HA_2 of $2,863 \text{ km}^2$, 962 km^2 , and 138 km^2 , respectively (Figure 6e4). Hypoxia was generated mainly in
the south of Lantau Island, with the minimum DO of 0.5 mg/L .

3.3 Spatial patterns of DO and low-oxygen conditions in the early autumn of the PRE

In addition to the summer season, low-oxygen conditions also existed in the early autumn in the PRE. Figure 8 shows
the DO distributions in September of 2001 and 2006. In general, DO displayed remarkable spatial variations in both



215 periods, but their distribution patterns as well as the location and severity of low-oxygen conditions were quite different. In September 2001, DO exhibited a northwest-southeast pattern at the surface (Figure 8a1) and a north-south pattern at the bottom (Figure 8b1). The DO content was relatively low on the eastern side of the PRE. The HA₄ in the surface water was estimated 345 km², while the HA₄ and HA₃ at the bottom were estimated 1,056 km² and 270 km², respectively.

220 In comparison, spatial variation of the surface DO in September 2006 was more significant, generally showing a northeast-southwest pattern with low DO at the near-shore and high DO at the open sea (Figure 8a2). Low-oxygen water almost covered the entire surface of the inner Lingdingyang Bay, and hypoxia (with DO as low as 1.1 mg/L) occurred in the upper region, with the HA₂ reaching 108 km²; the HA₄ and HA₃ were estimated 1,131 km² and 512 km², respectively. In regard to the bottom, most of the PRE was occupied by water low in oxygen, which extended
225 from the inner Lingdingyang Bay further to the western PRE and the southwest of Lantau Island (Figure 8b2). The estimated HA₂ reached 333 km², with the minimum DO of 0.8 mg/L, while the HA₄ and HA₃ reached 4,448 km² and 2,061 km², respectively.

4. Discussion

4.1 Mechanisms controlling the summertime low-oxygen conditions in the PRE

230 Our results demonstrate that the PRE has frequently experienced low-oxygen events in summer. For all the 22 summer months investigated (during 1976-2017), there were 21 records with low oxygen, 17 (accounting for 77%) with oxygen deficiency, and 5 (23%) with hypoxia, reflecting a feature of seasonal low oxygen and episodic hypoxia in the PRE. In addition to our study, there also have been many other reports on the low-oxygen and hypoxic events during the summer months, including June of 2001-2005, 2009-2010 and 2015; July of 2000, 2003-2004 and 2010; and August of
235 2001-2002, 2005, 2007, 2010-2011 and 2017 (Zhai et al., 2005; Yang et al., 2011; Huang et al., 2012; Ye et al., 2013; Li et al., 2018; Qian et al., 2018; Li et al., 2020; Cui et al., 2019).

For the PRE, the formation and development of low-oxygen conditions is closely related to multiple factors including the Pearl River diluted water and its carrying terrestrial substances, local productivity, vertical stratification intensity, water residence time, and topography. Specifically, the increased water temperature in summer (Figure 2)
240 could result in notable decrease of oxygen solubility in water and accelerated oxygen consumption by microbial respiration (Breitburg et al., 2018). In addition, the runoff was also increasing, with the summertime discharge approaching 16,500 m³/s (Figure 9). Massive freshwater inputs formed a distinct plume structure at the surface (Figure 10a1) together with the intrusion of high-salinity bottom waters along the deep navigation channel (Figure 10a2). This two-layer circulation driven by the density gradient (Wong et al., 2003) largely determines the distributions of
245 biochemical components and the subsequent development of low-oxygen conditions in the PRE. As shown in Table 2,



the bottom DO in summer had a significantly negative correlation with the vertical density difference ($r = -0.7131$, $p < 0.01$). This confirms that intense stratification was a critical physical setting for the generation and maintenance of bottom low-oxygen conditions, as denoted by previous studies (e.g., Rabouille et al., 2008; Li et al., 2020).

In the stratified waters (Figure 10a3), the bottom DO_s was comparatively low (Figure 10a4), implying the presence of significant oxygen consumption in the region. Multiple reports have manifested that sediment oxygen uptake was the dominant oxygen sink in the PRE and fueled primarily by the remineralization of organic matter accumulated in the sediments (Zhang and Li, 2010; Wang et al., 2017), which originated from terrestrial inputs and/or marine-sourced inputs through local production (Su et al., 2017; Ye et al., 2017). The dominance of terrestrial- and marine-sourced organic matter varied greatly in space. More specifically, a large fraction of terrestrial particulate matter settled on the sediments after entering the PRE (Hu et al., 2011) and ultimately experienced diagenetic decomposition by heterotrophic bacteria (Li et al., 2018), resulting in high oxygen demand (Wang et al., 2017; Lu et al., 2018). This was considered the primary cause for the low oxygen and sporadic hypoxic events observed in the shallow water east of Hengqin Island, the outer Modaomen Bay, and the deep channel (Figure 7b1-b2), where considerable deposition of organic matter and intense stratification occurred simultaneously (Hu et al., 2011). While in the offshore area of the PRE, water transparency improved due to the consecutive settling and dilution of suspended particles (Figure 10a5). On top of this, the relatively long residence time and rich nutrients carried by the river plume favor the growth and accumulation of phytoplankton biomass in the region. As shown in Figure 10a6, the chl *a* content was higher at the offshore than in the main estuary, especially on the eastern side where algae blooms and red tides have been frequently reported (Dai et al., 2008; Harrison et al., 2008) accompanied by supersaturated DO at the surface (Figures 3 and 5). Moreover, the offshore water of the eastern PRE is comparatively deep (> 15 m; Figure 1) and thus possessed a more stable profile of vertical stratification. The resulting restricted oxygen supply, coupled with the substantial delivery of labile organic matter from the surface water with phytoplankton blooms, made the coastal area from the southwest of Lantau Island to the northeast of Wanshan Islands vulnerable to frequent occurrence of low oxygen and episodic hypoxia (Figure 7b1-b2). The close linkage between the development of bottom low-oxygen conditions and nutrient-stimulated high productivity at the surface for this hotspot (hypoxia-prone) area has also been illustrated in several works (Su et al., 2017; Qian et al., 2018; Li et al., 2020), showing the dominant role of marine-sourced organic matter over the terrestrial inputs with respect to oxygen depletion. Moreover, under the control of the two-layer estuarine circulation, the local low-oxygen water generated in the lower estuary could be transported to the inner Lingdingyang Bay along the bottom of the deep channel (Cui et al., 2019; Li et al., 2020), which would further exacerbate the low-oxygen conditions in the bay.



4.2 Influential factors and underlying mechanisms of the low-oxygen conditions in the early autumn

In contrast to summer, there were very few studies concerning the problem of low-oxygen conditions in the early autumn of the PRE. Although Qian et al. (2018) discovered the existence of low oxygen in the waters adjacent to Humen as well as Hengqin Island and Lantau Island in September 2010, this issue did not attract much attention because the actual coverage and severity of low oxygen have not been fully unveiled owing to the small-scale field survey. Here the observations we used show prominent low-oxygen conditions in the early autumn (September) of 2001 and 2006 (both with the areal extent of low oxygen $> 1,000 \text{ km}^2$; Figure 8). In particular, over 100 km^2 and 330 km^2 of hypoxia were observed at the surface and bottom, respectively, in September 2006, which witnessed a hypoxic scale comparable to that of July 2014 (the period with the largest hypoxic area), a low-oxygen area very close to that of July 2015 (the period with the largest low-oxygen area), and an oxygen-deficiency extent that was significantly larger than those in all the summer months. Besides, it should be noted that the low-oxygen conditions in September 2006 were much more severe than those in the summer of 2006 (Figure 4b2), indicating that this issue was not a simple succession of the summer ones, but likely a spontaneous phenomenon that formed independently.

Unlike the summer, the freshwater discharge in September has decreased to approximately $10,000 \text{ m}^3/\text{s}$ (Figure 9), equivalent to $\sim 61\%$ of the summertime discharge, but it was still much larger than those in the mid-to-late autumn and winter. The drawdown of freshwater inputs led to weaker extension of the diluted water (Figure 10b1-b2) and smaller vertical density difference (Figure 10b3) compared with summer. The estuary was weakly stratified overall except for the waters from the outer Modaomen Bay to Wanshan Islands where moderate stratification was found. Table 2 shows that there was no significant correlation between the bottom DO and the vertical density difference in either September 2001 or September 2006. This implies that the mild stratification had a small effect on the low-oxygen conditions in early autumn, which seems to have a different underlying mechanism from that in summer.

As for September 2006, we speculate that the severe hypoxia occurring at the surface and bottom of the inner Lingdingyang Bay (Figure 8a2 and b2) resulted mainly from the inflows of low-oxygen waters from the upstream reaches, as evidenced by the significantly positive correlations between salinity and DO in Table 2 (with the correlation coefficients r reaching 0.7341 and 0.6637 at the surface and bottom, respectively, $p < 0.01$). Other factors including sewage effluents discharged from the runoff and coastal cities (as evidenced by the significant correlation between the surface DO and NH_4) and the respiration related to phytoplankton imported from the upstream reaches (as indicated by the high regional chl a contents in Figure 10b6; also in accordance with the finding by Ye et al. (2013)) supplement the maintenance of hypoxia. With respect to the waters from the middle part of the Lingdingyang Bay to the Modaomen Bay, marked low-oxygen conditions were largely restricted to the bottom (with DO_s ranging between 40% and 50%; Figure 10b4) and possibly controlled by a complex interplay of various processes. Since the river discharge has weakened compared with summer, a greater fraction of terrestrial organic matter would shift towards to



deposit at this area, while the water residence time became relatively longer (Sun et al., 2014) and thus favored the retention of organic matter and its eventual decomposition at the bottom. The influx of low-oxygen waters from the inner Lingdingyang Bay was an additional stressor that could also contribute to the substantial oxygen deficit in this region. Regarding the lower estuary, a large area of high phytoplankton biomass (with the maximum chl *a* content > 23 mg/m³) was observed (Figure 10b6) because of the good light condition attributed to the low concentrations of suspended particles (Figure 10b5). Meanwhile, the prolonged water residence time was conducive to the retention and degradation of organic matter supplied by the elevated primary production in the region, thus resulting in significant oxygen consumption and decline in the bottom water.

Overall, the combined actions of the upstream low-oxygen inflows and enhanced oxygen depletion driven by an intricate coupling of physical and biogeochemical processes eventually led to the emergency of large-scale (estuary-wide) low-oxygen event in September 2006. By contrast, the low-oxygen conditions were much less severe in September 2001 (Figure 8a1 and b1). This suggests that in the periods of early autumn, there was considerable interannual variability in the spatial extents and intensity of low-oxygen conditions, which has also been observed in summer. Plausible drivers for such interannual variability include the associated changes in freshwater discharge and wind forcing (both of which are the major factors controlling the spreading of the nutrient-rich river plume; Xu et al., 2019) as well as terrestrial material inputs (including organic matter, nutrients, and suspended particles), which could induce significant alterations to physical conditions (e.g., vertical density stratification and mixing, estuarine circulation, retention time) and internal production of organic matter. Further studies are needed to clarify the role of changes related to different dynamic factors in the generation and variations of low-oxygen conditions in the PRE.

4.3 Long-term expansions of low-oxygen and hypoxic areas in the PRE

The global ocean and coastal waters have been experiencing notable oxygen declines over the past several decades, with significant increases in the number and severity of hypoxic areas in recent years (Breitburg et al., 2018; Diaz and Rosenberg, 2008). This rapid oxygen loss is largely attributed to intensive anthropogenic activities that have caused global warming and nutrient enrichment of coastal waters. Apparent long-term expansions of hypoxic conditions have been documented in several coastal systems, e.g., the Baltic Sea, where the hypoxic volume has expanded dramatically with increasing nutrient inputs from its watershed and enhanced water-column respiration resulting from warming (Fennel and Testa, 2019 and references therein); the northern Gulf of Mexico, Chesapeake Bay, and the Yangtze River estuary, all of which experience sustained seasonal hypoxia that has shown significant enlargement in spatial extents in response to anthropogenic eutrophication (Bianchi et al., 2010; Murphy et al., 2011; Zhu et al., 2011).

It is commonly recognized that the PRE did not develop similar large-scale, persistent low-oxygen zone as in other hypoxic systems (e.g., the northern Gulf of Mexico, the Yangtze River estuary). A combination of intriguing



features including shallow and turbid waters, rapid physical exchanges, and unstable vertical stratification provides
340 good buffering capacity for the PRE to mitigate eutrophication and hypoxic conditions in summer. Moreover, the
freshwater input was characterized with excess nitrogen (N) and low phosphorus (P), yielding an N: P ratio beyond
100 (Harrison et al., 2008; Hu and Li, 2009). Therefore, the growth of phytoplankton was heavily inhibited over a
large area of the PRE due to strong phosphorus limitation, together with high water turbidity (Figure 10a5) and short
residence time (Sun et al., 2014). However, with the rapidly changing environments in recent years, the summertime
345 low-oxygen conditions in the PRE has undergone an apparent expansion in areal extents, as indicated in Figures 4 and
6; large extents of low oxygen, oxygen deficiency, and hypoxia exceeding 4,450 km², 1,120 km², and 330 km²,
respectively, were present during 2014-2017. This emerging declining trend of bottom oxygen and spatial expansion of
low-oxygen conditions in the PRE have been supported by previous studies (Ye et al., 2012; Qian et al., 2018). By
analyzing the sediment cores in the PRE, Ye et al. (2012) discovered that due to the influence of human activities,
350 eutrophic conditions in the estuary have been exacerbated since the 1970s, and the relative abundance of hypoxia-
resistant foraminifera has substantially increased, implying that the DO conditions in the bottom waters were
deteriorating. Based on the monitoring data collected by the Hong Kong Environmental Protection Agency from a
coastal site (SM18) during 1990-2014, Qian et al. (2018) also identified a significant decrease in the bottom DO over
the past 25 years. Collectively, the results from our study and previous research described above have consistently
355 corroborated the gradual exacerbation of low-oxygen conditions in the PRE. Besides, the years around 2000 appear to
be a key time node for the emergence of apparent deoxygenation, which coincided with the sharp environment changes
along with the growing economics and populations in China.

Firstly, the long-term decline of oxygen was thought to be principally driven by the increasing wastewater
discharge in the Pearl River Delta region. As shown in Figure 11a, the annual wastewater discharge in Guangdong
360 Province has increased from ~2.5 billion tons in 1990 to ~9.4 billion tons in 2016, thereby resulting in remarkable
nutrient enrichment and water quality deterioration. According to Li et al. (2020), nutrient concentrations in the
upstream reaches, which received a large amount of sewage effluents from Guangzhou and Dongguan, were mostly
higher than 50 µg/L for NH₄, 1000 µg/L for NO₃, and 30 µg/L for PO₄ since 2000, coincident with the accelerated
growth of wastewater discharge (Figure 11a). The elevated nutrients, especially PO₄, which almost doubled from the
365 1990s to the 2010s (Li et al., 2020), would very likely promote the phytoplankton biomass and local production of
organic matter in the PRE; indeed, Li et al. (2020) reported an increasing trend of chl *a* in the surface waters of the
lower estuary from 2001 to 2011, with concentrations exceeding 10 µg/L in recent years. Furthermore, as a result of
intense nitrification and aerobic respiration of organic matter from direct anthropogenic inputs (He et al., 2014), the
DO content in the upstream reaches has been declining since 1998, with periodic low oxygen and episodic hypoxia
370 starting from 2000 (Li et al., 2020). Therefore, the inflows from the upstream reaches preconditioned the freshwater



delivering into the PRE with increasingly high levels of nutrients and organic matter as well as low-oxygen waters, which had significant contributions to the low DO levels in the inner Lingdingyang Bay since 1999 (Figures 5-6).

Secondly, in addition to the continued rise in nutrients and various pollutants, dramatic alterations to water discharge and sediment load were identified as well because of the combined effects of global climate change and regional high-intensity human activities (e.g., the construction of dams and reservoirs, soil-water conservation measures, altered land-use patterns). As recently reported by Wu et al. (2020), the sediment load of the nine major rivers (including the Yangtze, Pearl, and Yellow rivers) in China has dramatically dropped by 85% over the past six decades, and the year 1999 was identified as one of the important time nodes for the sediment declines. As for the Pearl River, its water discharge showed a slight downward trend during 1979-2015 (Figure 11b); however, the sediment load was characterized with a more significant decline (Figure 11c), approximately by 63% between 1979-1998 (~85 million tons/a) and 1999-2015 (~31 million tons/a) primarily attributed to anthropogenic impacts (Wu et al., 2020). One potential consequence of this abrupt change was that the PRE would become more susceptible to widespread eutrophication and strengthened oxygen depletion as the light shading effect of suspended sediments on primary production was greatly weakened. With respect to other stressors, including ocean warming and upwelling of subsurface low-oxygen, nutrient-rich waters from the South China Sea, it has been clarified that they had minor contributions to the observed long-term decline of oxygen in the PRE (Qian et al., 2018).

4.4 Implication and limitations

By using the field observations over 42 years, this study is a first attempt to reveal the long-term evolution of low-oxygen conditions in the PRE in terms of spatial extents. Although there existed data gaps in certain years and lack of conformity in observational coverage, the observations witnessed a distinct exacerbation of summertime low-oxygen conditions as the increased frequencies in extremes (e.g. $HA_4 > 1,600 \text{ km}^2$). In the context of global oxygen declines, unveiling this potential decadal change in low-oxygen conditions could be helpful for us to project and better understand the future oxygen status in the PRE as well as other coastal systems subject to intense anthropogenic disturbances. In addition, our results also identified two prominent low-oxygen events in the early autumn of the PRE, which were not inherited from summer ones but formed by different mechanisms. Given the insufficient attention to this issue so far, our finding is not merely a supplement to the understanding of oxygen dynamics in the PRE, but also a critical reminder to realize the importance and severity of the low-oxygen problem in early autumn. It is highly essential to strengthen scientific research and field investigations on this issue in order to fully elucidate its current status, formation process, and controlling factors, especially in the context of the spatial expansions of low-oxygen conditions observed in summer.



Nevertheless, a caveat to the historical observations for the PRE is that they were under sampled in some years, especially before the 2010s. This would largely limit our abilities to quantify the long-term changes in low-oxygen conditions and to further investigate the associated mechanisms. For instance, low oxygen was observed in some summer months (Figure 6), e.g. July 1992, July 1994, and August 1999; however, we were unable to estimate their coverage and intensity due to the lack of sufficient observations. To this end, we would like to emphasize the urgency of conducting estuary-wide surveys to collect more extensive data on DO and its related factors in the PRE. Furthermore, we could merge the in-situ observations into sophisticated numerical models through model calibration and/or data assimilation to provide a more thorough insight into the temporal and spatial variability, development, and underlying processes of low-oxygen conditions in the PRE.

410 5. Conclusion

This study explores the long-term spatiotemporal variations of DO as well as the locations and severity of low-oxygen conditions in the PRE by utilizing a collection of observations during 1976-2017. Our analysis has revealed a number of important aspects concerning the low-oxygen status (including the hotspots with high incidence of low-oxygen events) and the associated long-term changes over the past 42 years. The spatial patterns of DO and low-oxygen conditions exhibited significant seasonal, intra-seasonal, and interannual variations. Low-oxygen conditions were frequently observed in summer and primarily present in the bottom waters affected by intense vertical stratification and oxygen uptake by the sediments. Furthermore, the summertime low-oxygen conditions have experienced an apparent expansion in spatial extents over recent years. The synergetic effects of substantially increased loads of anthropogenic nutrients and organic matter, sharply decreased load of suspended sediments, and direct inflows of low-oxygen waters from the Pearl River act to promote the exacerbation of low-oxygen conditions in the PRE. Prominent low-oxygen events were also present in early autumn, showing different characteristics and underlying mechanisms from those in summer. To sum up, our results indicate that the PRE could form large areas of low oxygen under proper environmental conditions, as exemplified in September 2006 and the summer months of 2014-2017, and that this river-dominated estuary has shown a clear trend of developing into a seasonal, estuary-wide oxygen-deficiency/hypoxic zone.



Data availability. The in-situ observations in use are available upon request.

Author contributions. **Jiatang Hu:** Conceptualization, data analysis, drafting, review & editing. **Zhongren Zhang:** Graphic visualization, review & editing. **Bin Wang:** Writing & review. **Jia Huang:** Data compilation & analysis.

Declaration of competing interests. The authors declare that they have no known competing financial interests or
430 personal relationships that could have appeared to influence the work reported in this paper.

Acknowledges. This work was supported by the Joint Research Fund of the National Natural Science Foundation of China and Guangdong Province (U1901209).

References

- Bianchi, T. S., DiMarco, S. F., Cowan, J. H., Hetland, R. D., Chapman, P., Day, J. W., and Allison, M. A.: The science of
435 hypoxia in the Northern Gulf of Mexico: A review, *Science of the Total Environment*, 408, 1471-1484,
<https://doi.org/10.1016/j.scitotenv.2009.11.047>, 2010.
- Breitburg, D., Levin, L. A., Oschlies, A., Grégoire, M., Chavez, F. P., Conley, D. J., Garçon, V., Gilbert, D., Gutiérrez, D.,
Isensee, K., Jacinto, G. S., Limburg, K. E., Montes, I., Naqvi, S. W. A., Pitcher, G. C., Rabalais, N. N., Roman, M. R.,
440 Rose, K. A., Seibel, B. A., Telszewski, M., Yasuhara, M., and Zhang, J.: Declining oxygen in the global ocean and
coastal waters, *Science*, 359, 1-13, <https://doi.org/10.1126/science.aam7240>, 2018.
- Cai, W. J., Hu, X., Huang, W. J., Murrell, M. C., Lehrter, J. C., Lohrenz, S. E., Chou, W. C., Zhai, W., Hollibaugh, J. T.,
Wang, Y., Zhao, P., Guo, X., Gundersen, K., Dai, M., and Gong, G. C.: Acidification of subsurface coastal waters
enhanced by eutrophication, *Nature Geoscience*, 4, 766-770, <https://doi.org/10.1038/ngeo1297>, 2011.
- Chen, J. C., Heinke, G. W., and Zhou, M. J.: The Pearl River Estuary Pollution Project (PREPP), *Continental Shelf Research*,
445 24, 1739-1744, <https://doi.org/10.1016/j.csr.2004.06.004>, 2004.
- Cui, Y., Wu, J., Ren, J., and Xu, J.: Physical dynamics structures and oxygen budget of summer hypoxia in the Pearl River
Estuary, *Limnology and Oceanography*, 64, 131-148, <https://doi.org/10.1002/lno.11025>, 2019.
- Dai, M., Zhai, W., Cai, W.-J., Callahan, J., Huang, B., Shang, S., Huang, T., Li, X., Lu, Z., Chen, W., and Chen, Z.: Effects
450 of an estuarine plume-associated bloom on the carbonate system in the lower reaches of the Pearl River estuary and the
coastal zone of the northern South China Sea, *Continental Shelf Research*, 28, 1416-1423,
<https://doi.org/10.1016/j.csr.2007.04.018>, 2008.
- Diaz, R. J., and Rosenberg, R.: Spreading Dead Zones and Consequences for Marine Ecosystems, *Science*, 321, 926-929,
<https://doi.org/10.1126/science.1156401>, 2008.
- Feng, Y., Fennel, K., Jackson, G. A., Dimarco, S. F., and Hetland, R. D.: A model study of the response of hypoxia to
455 upwelling-favorable wind on the northern Gulf of Mexico shelf, *Journal of Marine Systems*, 131, 63-73,
<https://doi.org/10.1016/j.jmarsys.2013.11.009>, 2014.



- Fennel, K., and Testa, J. M.: Biogeochemical Controls on Coastal Hypoxia, *Annual Review of Marine Science*, 11, 105-130, <https://doi.org/10.1146/annurev-marine-010318-095138>, 2019.
- Harrison, P. J., Yin, K., Lee, J. H. W., Gan, J., and Liu, H.: Physical-biological coupling in the Pearl River Estuary, *Continental Shelf Research*, 28, 1405-1415, <https://doi.org/10.1016/j.csr.2007.02.011>, 2008.
- 460 He, B., Dai, M., Zhai, W., Guo, X., and Wang, L.: Hypoxia in the upper reaches of the Pearl River Estuary and its maintenance mechanisms: A synthesis based on multiple year observations during 2000–2008, *Marine Chemistry*, 167, 13-24, <https://doi.org/10.1016/j.marchem.2014.07.003>, 2014.
- Hu, J., and Li, S.: Modeling the mass fluxes and transformations of nutrients in the Pearl River Delta, China, *Journal of*
465 *Marine Systems*, 78, 146-167, <https://doi.org/10.1016/j.jmarsys.2009.05.001>, 2009.
- Hu, J., Li, S., and Geng, B.: Modeling the mass flux budgets of water and suspended sediments for the river network and estuary in the Pearl River Delta, China, *Journal of Marine Systems*, 88, 252-266, <https://doi.org/10.1016/j.jmarsys.2011.05.002>, 2011.
- Huang, X., Lin, J., Zhang, S., and Liang, K.: The distribution of seawater chemical elements in Pearl River Estuary and
470 seawater quality assessment, *Transactions of Oceanology and Limnology*, 162-174, <https://doi.org/10.13984/j.cnki.cn37-1141.2012.03.023>, 2012. (in Chinese with English abstract)
- Hyer, P. V., Fang, C. S., Ruzicki, E. P., and Hargis, W. J.: Hydrography and Hydrodynamics of Virginia Estuaries II: Studies of the Distribution of Salinity and Dissolved Oxygen in the Upper York System, Virginia Institute of Marine Science, College of William and Mary, America, 1971.
- 475 Li, G., Liu, J., Diao, Z., Jiang, X., Li, J., Ke, Z., Shen, P., Ren, L., Huang, L., and Tan, Y.: Subsurface low dissolved oxygen occurred at fresh- and saline-water intersection of the Pearl River estuary during the summer period, *Marine Pollution Bulletin*, 126, 585-591, <https://doi.org/10.1016/j.marpolbul.2017.09.061>, 2018.
- Li, X., Lu, C., Zhang, Y., Zhao, H., Wang, J., Liu, H., and Yin, K.: Low dissolved oxygen in the Pearl River estuary in summer: Long-term spatio-temporal patterns, trends, and regulating factors, *Marine Pollution Bulletin*, 151, 110814, <https://doi.org/10.1016/j.marpolbul.2019.110814>, 2020.
- 480 Lin, H., Liu, S., and Han, W.: Potential trigger CTB, from seasonal bottom water hypoxia in the Pearl River Estuary, *Journal of Zhanjiang Ocean University*, 21, 25-29, 2001. (in Chinese with English abstract)
- Lu, Z., Gan, J., Dai, M., Liu, H., and Zhao, X.: Joint Effects of Extrinsic Biophysical Fluxes and Intrinsic Hydrodynamics on the Formation of Hypoxia West off the Pearl River Estuary, *Journal of Geophysical Research: Oceans*, 123, 6241-6259, <https://doi.org/10.1029/2018JC014199>, 2018.
- 485 Luo, L., Li, S., and Wang, D.: Hypoxia in the Pearl River Estuary, the South China Sea, in July 1999, *Aquatic Ecosystem Health & Management*, 12, 418-428, <https://doi.org/10.1080/14634980903352407>, 2009.
- Middelburg, J. J., and Levin, L. A.: Coastal hypoxia and sediment biogeochemistry, *Biogeosciences*, 6, 1273-1293, <https://doi.org/10.5194/bg-6-1273-2009>, 2009.



- 490 Murphy, R. R., Kemp, W. M., and Ball, W. P.: Long-Term Trends in Chesapeake Bay Seasonal Hypoxia, Stratification, and
Nutrient Loading, *Estuaries and Coasts*, 34, 1293-1309, <https://doi.org/10.1007/s12237-011-9413-7>, 2011.
- Qian, W., Gan, J., Liu, J., He, B., Lu, Z., Guo, X., Wang, D., Guo, L., Huang, T., and Dai, M.: Current status of emerging
hypoxia in a eutrophic estuary: The lower reach of the Pearl River Estuary, China, *Estuarine, Coastal and Shelf Science*,
205, 58-67, <https://doi.org/10.1016/j.ecss.2018.03.004>, 2018.
- 495 Rabalais, N. N., Turner, R. E., and Jr., W. J. W.: Gulf of Mexico Hypoxia, A.K.A. “The Dead Zone”, *Annual Review of
Ecology and Systematics*, 33, 235-263, <https://doi.org/10.1146/annurev.ecolsys.33.010802.150513>, 2002.
- Rabalais, N. N., Díaz, R. J., Levin, L. A., Turner, R. E., Gilbert, D., and Zhang, J.: Dynamics and distribution of natural and
human-caused hypoxia, *Biogeosciences*, 7, 585-619, <https://doi.org/10.5194/bg-7-585-2010>, 2010.
- Rabouille, C., Conley, D. J., Dai, M. H., Cai, W. J., Chen, C. T. A., Lansard, B., Green, R., Yin, K., Harrison, P. J., Dagg, M.,
500 and McKee, B.: Comparison of hypoxia among four river-dominated ocean margins: The Changjiang (Yangtze),
Mississippi, Pearl, and Rhne rivers, *Continental Shelf Research*, 28, 1527-1537,
<https://doi.org/10.1016/j.csr.2008.01.020>, 2008.
- Shi, Z., Liu, K., Zhang, S., Xu, H., and Liu, H.: Spatial distributions of mesozooplankton biomass, community composition
and grazing impact in association with hypoxia in the Pearl River Estuary, *Estuarine Coastal & Shelf Science*, 225,
505 106237.106231-106237.106210, <https://doi.org/10.1016/j.ecss.2019.05.019>, 2019.
- Su, J., Dai, M., He, B., Wang, L., Gan, J., Guo, X., Zhao, H., and Yu, F.: Tracing the origin of the oxygen-consuming
organic matter in the hypoxic zone in a large eutrophic estuary: the lower reach of the Pearl River Estuary, China,
Biogeosciences Discussions, 14, 4085-4099, <https://doi.org/10.5194/bg-14-4085-2017>, 2017.
- Sun, J., Lin, B., Li, K., and Jiang, G.: A modelling study of residence time and exposure time in the Pearl River Estuary,
510 China, *Journal of Hydro-environment Research*, 8, 281-291, <https://doi.org/10.1016/j.jher.2013.06.003>, 2014.
- Wang, B., Hu, J., Li, S., and Liu, D.: A numerical analysis of biogeochemical controls with physical modulation on hypoxia
during summer in the Pearl River estuary, *Biogeosciences*, 14, 2979-2999, <https://doi.org/10.5194/bg-14-2979-2017>,
2017.
- Wei, Q. S., Wang, B. D., Zhigang, Y. U., Chen, J. F., and Xue, L.: Mechanisms leading to the frequent occurrences of
515 hypoxia and a preliminary analysis of the associated acidification off the Changjiang estuary in summer, *Science
China(Earth Sciences)*, 60, 360-381, <https://doi.org/10.1007/s11430-015-5542-8>, 2017.
- Wong, L. A., Chen, J., Xue, H., Dong, L. X., Su, J. L., and Heinke, G.: A model study of the circulation in the Pearl River
Estuary (PRE) and its adjacent coastal waters: 1. Simulations and comparison with observations, *Journal of
Geophysical Research-Oceans*, 108, <https://doi.org/10.1029/2002jc001451>, 2003.
- 520 Wu, Z., Zhao, D., Syvitski, J. P. M., Saito, Y., and Wang, M.: Anthropogenic impacts on the decreasing sediment loads of
nine major rivers in China, 1954–2015, *Science of the Total Environment*, 739, 1-21,
<https://doi.org/10.1016/j.scitotenv.2020.139653>, 2020.



- Xu, C., Xu, Y. J., Hu, J. T., Li, S. Y., and Wang, B.: A numerical analysis of the summertime Pearl River plume from 1999 to 2010: Dispersal patterns and intraseasonal variability, *Journal of Marine Systems*, 192, 15-27, <https://doi.org/10.1016/j.jmarsys.2018.12.010>, 2019.
- Yang, W., Luo, L., Gao, Y., Zu, T., and Wang, D.: Comparison of environmental constituents in the Pearl River Estuary during summer of 1999 and 2009, *Journal of Tropical Oceanography*, 30, 16-23, 2011. (in Chinese with English abstract)
- Ye, F., Huang, X., Zhang, X., Zhang, D., Zeng, Y., and Tian, L.: Recent oxygen depletion in the Pearl River Estuary, South China: geochemical and microfaunal evidence, *Journal of Oceanography*, 68, 387-400, <https://doi.org/10.1007/s10872-012-0104-1>, 2012.
- Ye, F., Huang, X., Shi, Z., and Liu, Q.: Distribution characteristics of dissolved oxygen and its affecting factors in the Pearl River Estuary during the summer of the extremely drought hydrological year 2011, *Environmental Science*, 34, 2013.
- Ye, F., Guo, W., Shi, Z., Jia, G., and Wei, G.: Seasonal dynamics of particulate organic matter and its response to flooding in the Pearl River Estuary, China, revealed by stable isotope ($\delta^{13}\text{C}$ and $\delta^{15}\text{N}$) analyses, *Journal of Geophysical Research: Oceans*, 122, <https://doi.org/10.1002/2017JC012931>, 2017.
- Yin, K., Lin, Z., and Ke, Z.: Temporal and spatial distribution of dissolved oxygen in the Pearl River Estuary and adjacent coastal waters, *Continental Shelf Research*, 24, 1935-1948, <https://doi.org/10.1016/j.csr.2004.06.017>, 2004.
- Yu, L., Fennel, K., and Laurent, A.: A modeling study of physical controls on hypoxia generation in the northern Gulf of Mexico, *Journal of Geophysical Research Oceans*, 120, 5019-5039, <https://doi.org/10.1002/2014JC010634>, 2015.
- Zhai, W., Dai, M., Cai, W. J., Wang, Y., and Wang, Z.: High partial pressure of CO_2 and its maintaining mechanism in a subtropical estuary: the Pearl River estuary, China, *Marine Chemistry*, 93, 21-32, <https://doi.org/10.1016/j.marchem.2004.07.003>, 2005.
- Zhang, H., and Li, S.: Effects of physical and biochemical processes on the dissolved oxygen budget for the Pearl River Estuary during summer, *Journal of Marine Systems*, 79, 65-88, <https://doi.org/10.1016/j.jmarsys.2009.07.002>, 2010.
- Zhang, J., Gilbert, D., Gooday, A. J., Levin, L., Naqvi, S. W. A., Middelburg, J. J., Scranton, M., Ekau, W., Peña, A., Dewitte, B., Oguz, T., Monteiro, P. M. S., Urban, E., Rabalais, N. N., Ittekkot, V., Kemp, W. M., Ulloa, O., Elmgren, R., Escobar-Briones, E., and Van der Plas, A. K.: Natural and human-induced hypoxia and consequences for coastal areas: synthesis and future development, *Biogeosciences*, 7, 1443-1467, <https://doi.org/10.5194/bg-7-1443-2010>, 2010.
- Zhang, W., Wu, H., and Zhu, Z.: Transient Hypoxia Extent Off Changjiang River Estuary due to Mobile Changjiang River Plume, *Journal of Geophysical Research Oceans*, 123, 9196-9211, <https://doi.org/10.1029/2018JC014596>, 2018.
- Zhu, Z.-Y., Zhang, J., Wu, Y., Zhang, Y.-Y., Lin, J., and Liu, S.-M.: Hypoxia off the Changjiang (Yangtze River) Estuary: Oxygen depletion and organic matter decomposition, *Marine Chemistry*, 125, 108-116, <https://doi.org/10.1016/j.marchem.2011.03.005>, 2011.



Tables

Table 1. A summary of the observational data in the PRE used for analysis.

Dataset	Time period	Data in use
(1)	spring (March of 1985, 1987, and 1989-1997; April 2006) summer (August 1976; July of 1985, 1987, and 1989-1997; August 1999; July 2005; August 2009) autumn (November 1976; October of 1985, 1987, and 1989-1997; September of 2001 and 2006) Winter (February 1978)	Temperature (T), salinity (S), dissolved oxygen (DO), suspended sediment concentrations (SSC), ammonia (NH ₄), nitrate (NO ₃), phosphate (PO ₄), and chlorophyll (chl) <i>a</i> * in the surface and bottom waters
(2)	summer (July 1999)	Surface and bottom T, S, DO, SSC, NH ₄ , NO ₃ , PO ₄ , and chl <i>a</i>
(3)	spring (April 2007); summer (July-August 2006); autumn (October-November 2007); winter (December 2006-January 2007)	Surface and bottom T, S, and DO
(4)	spring (May 2014); summer (August 2013); autumn (November 2013); winter (February 2014)	Surface and bottom T, S, DO, SSC, NH ₄ , NO ₃ , and PO ₄
(5)	summer (July of 2014, 2015, and 2017)	Bottom DO

Data sources: (1) 42 cruises conducted by the South China Sea Environmental Monitoring Center during 1976-2006; (2) a summer cruise conducted by the Pearl River Estuary Pollution Project; (3) 4 seasonal cruises conducted by the State Oceanic Administration of China during 2006-2007; (4) 4 seasonal cruises conducted the Marine and Fishery Environmental Monitoring Center of Guangdong Province during 2013-2014; (5) data adopted from the literatures (Su et al., 2017; Lu et al., 2018; Shi et al., 2019).

* Note that in dataset (1) chl *a* data was only available for September 2006.

560



Table 2. Pearson correlation coefficients (*r*) between DO and other water quality metrics

Time period		S	T	$\Delta\rho$	NH ₄	NO ₃	PO ₄	chl <i>a</i>
Summer	Surface	0.2082**	-0.0043	0.2820**	-0.3188**	-0.3939**	-0.6153**	0.6788**
	Bottom	-0.5977**	0.4292**	-0.7131**	0.1109	0.2926**	-0.1421	0.4035*
Sep 2006	Surface	0.7341**	-0.3000	0.6783**	-0.4910*	-0.8052**	-0.2742	0.4314
	Bottom	0.6637**	-0.6703**	0.4582	0.0417	-0.6693**	-0.3513	-0.6077**
Sep 2001	Surface	0.0394	-0.0989	0.1424	-0.5686*	0.1554	-0.5381*	NA
	Bottom	-0.2953	0.3261	-0.1002	-0.4612	0.3292	-0.4097	NA

565 Notes: (1) $\Delta\rho$ represents the difference of density between the surface and bottom waters (bottom density minus surface density); (2) **
 indicates significance correlations at $p < 0.01$, and * indicates significant correlations at $p < 0.05$.

570

575

580

585

590



Figures

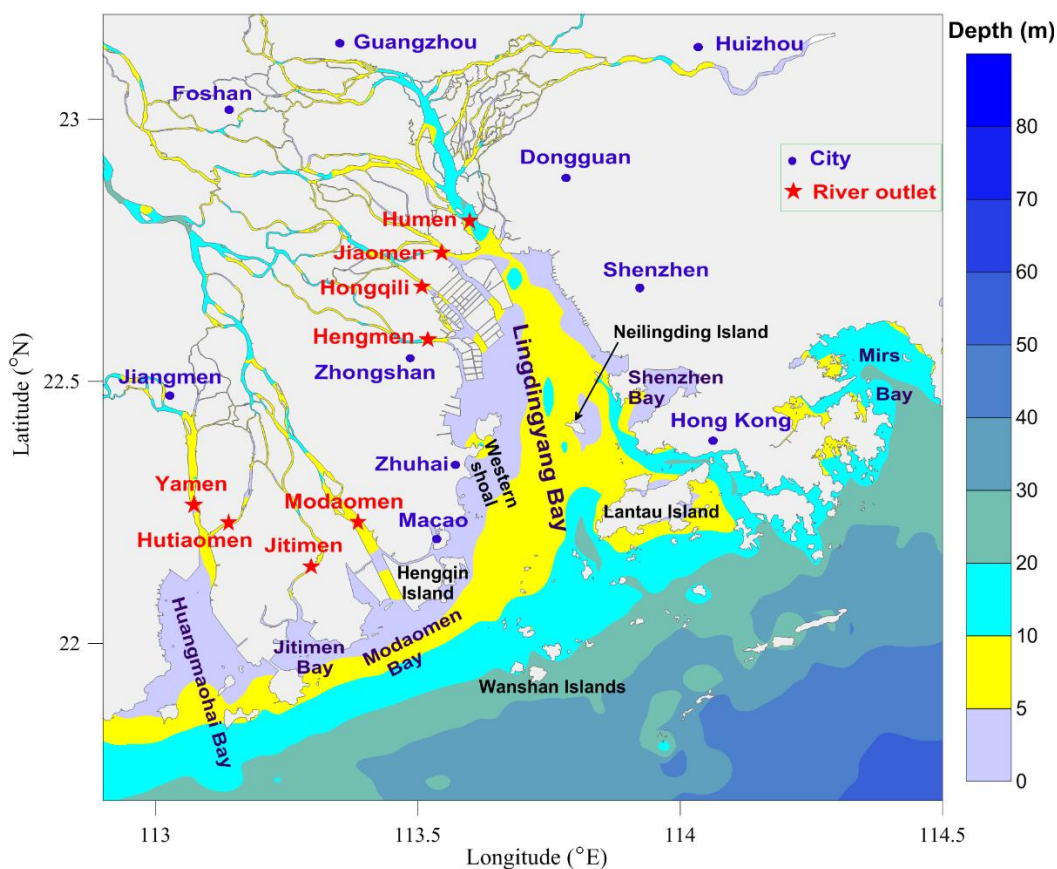


Figure 1. Map of the Pearl River estuary (PRE) and adjacent coastal waters. Note that the blue dots denote cities in the Guangdong-Hong Kong-Macao Greater Bay Area, and the red stars indicate the locations of eight outlets of the Pearl River freshwater discharged into the PRE; Humen, Jiaomen, Hongqili, and Hengmen are typically called the eastern four river outlets, while the others are called the western four river outlets.

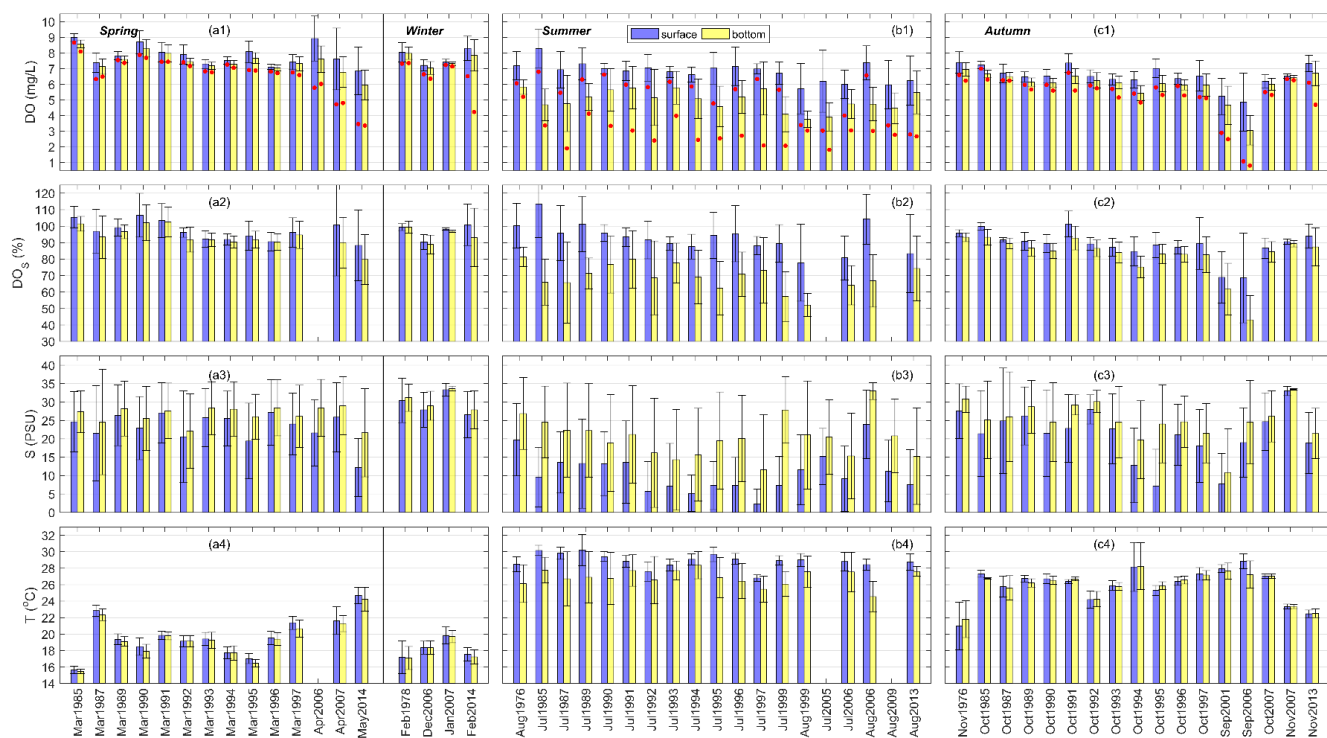


Figure 2. Spatial means and standard deviations of DO concentrations, DO saturation (DO_s), salinity (S), and temperature (T) in the surface and bottom waters of the PRE in (a) spring (March-May) and winter (December-February), (b) summer (June-August), and (c) autumn (September-November) during 1976-2014. Note that the red dots in the first row of the figure represent the lowest DO values measured in each time period.

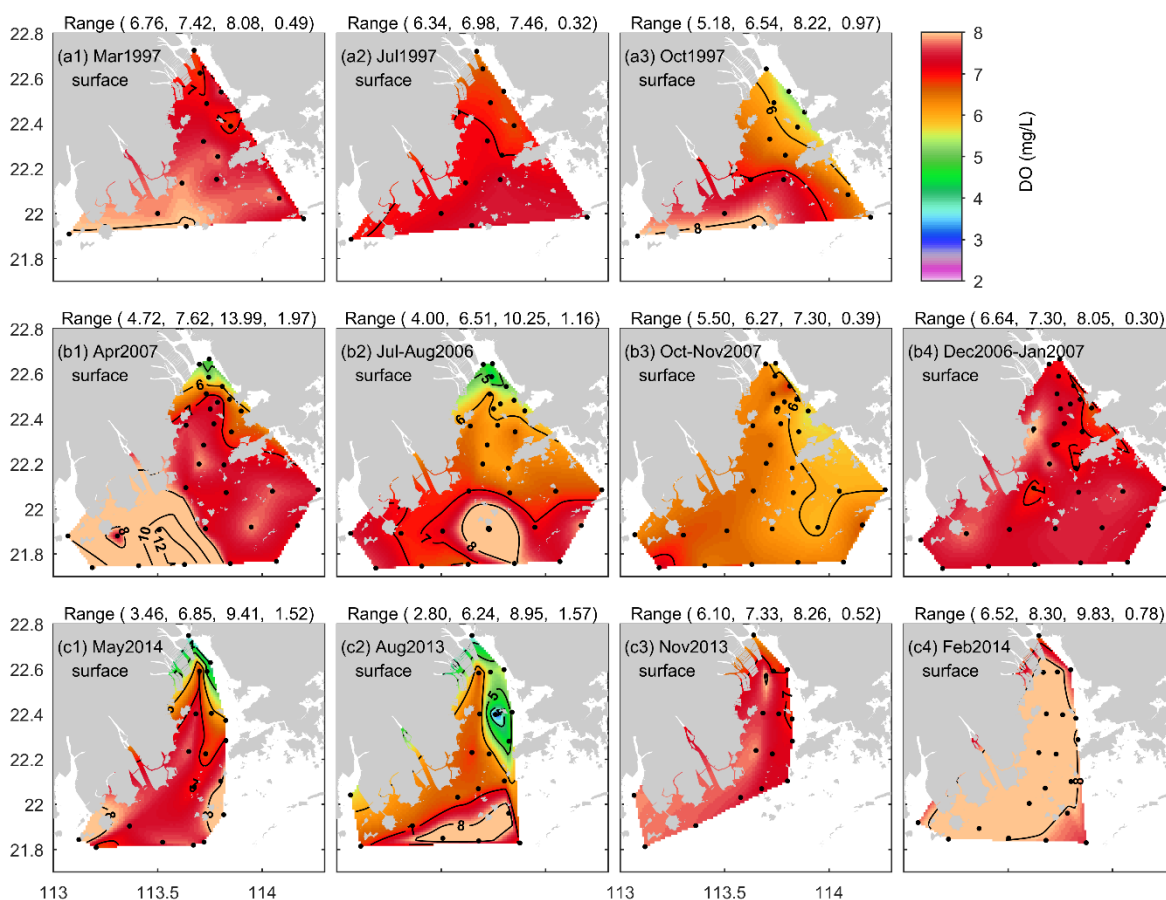


Figure 3. Seasonal variations of surface DO distributions in the PRE for (a) 1997, (b) 2006-2007, and (c) 2013-2014. The first to last columns of the figure correspond to spring, summer, autumn, and winter, respectively. Note that the numbers in brackets in the titles are the minimum, mean, maximum, and standard deviation values of DO in sequence; the black dots show the locations of the sampling stations.



610

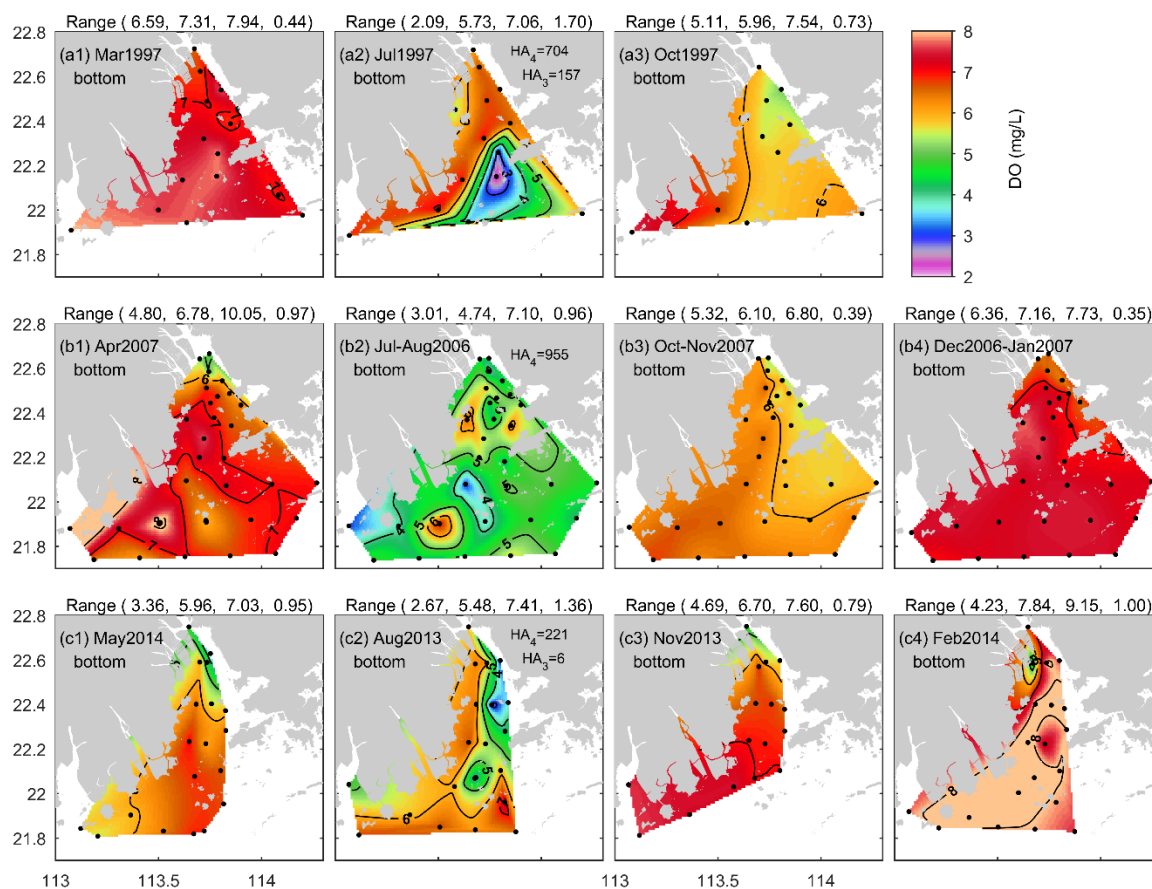


Figure 4. Same as Figure 3 but for the bottom water. Note that HA_4 , HA_3 , and HA_2 represent the areal extents (km^2) with $\text{DO} < 4$, 3, and 2 mg/L estimated from the available monitoring data, respectively.

615

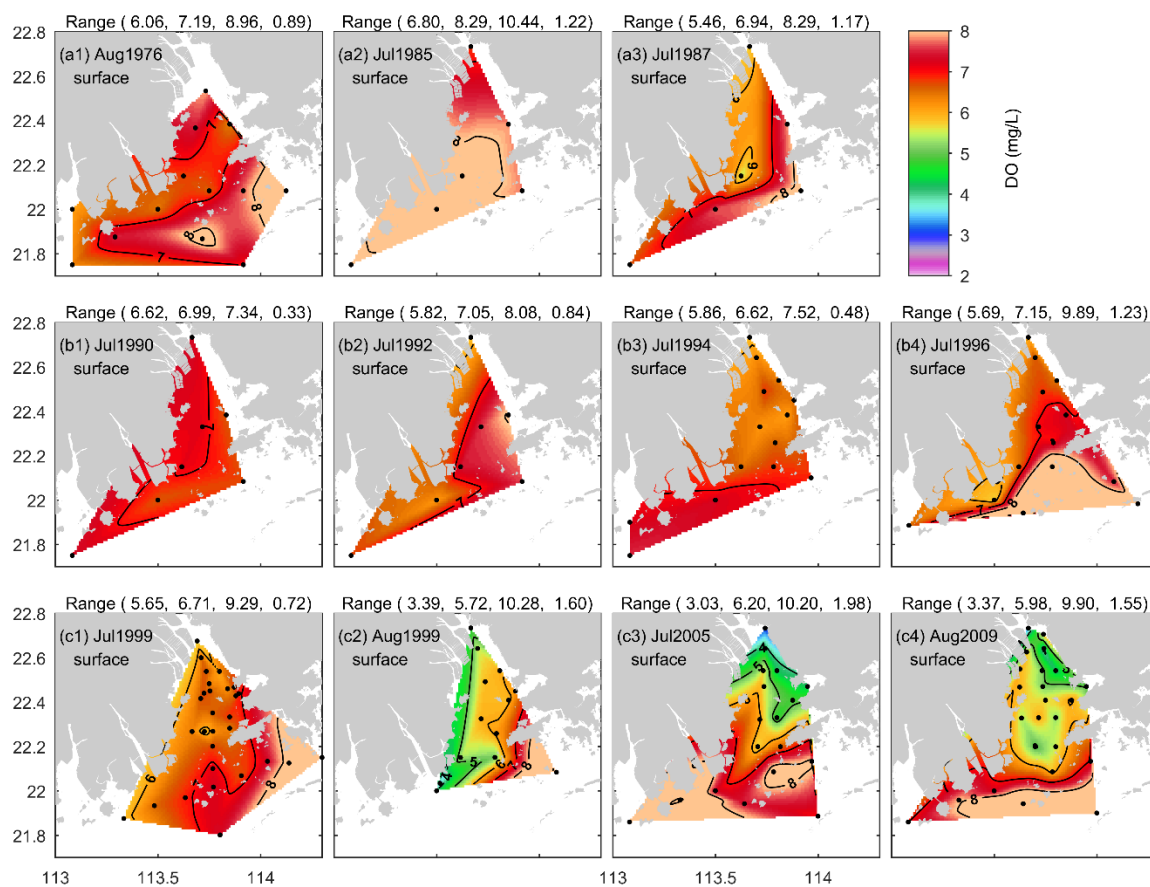


Figure 5. DO distributions at the surface of the PRE in summer.

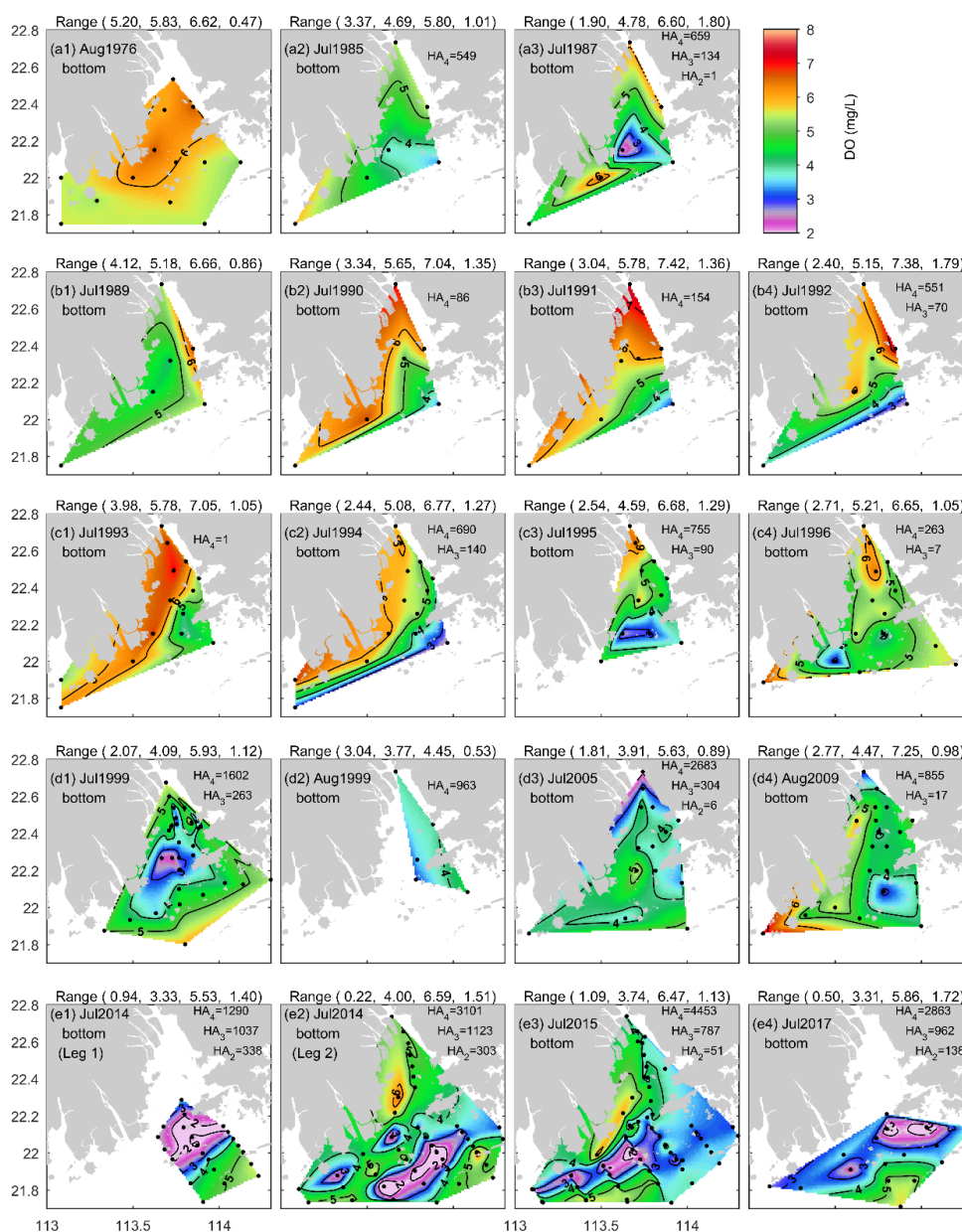


Figure 6. DO distributions at the bottom of the PRE for the summer months of 1976-2017. Due to the influence of Typhoon Rammasun, the cruise in July 2014 was divided into two legs, including (e1) Leg 1 in 13-16 July and (e2) Leg 2 in 19-27 July (Su et al., 2017). Note that HA₄, HA₃, and HA₂ represent the observation-based estimates of the areal extents (km²) with DO < 4, 3, and 2 mg/L, respectively.

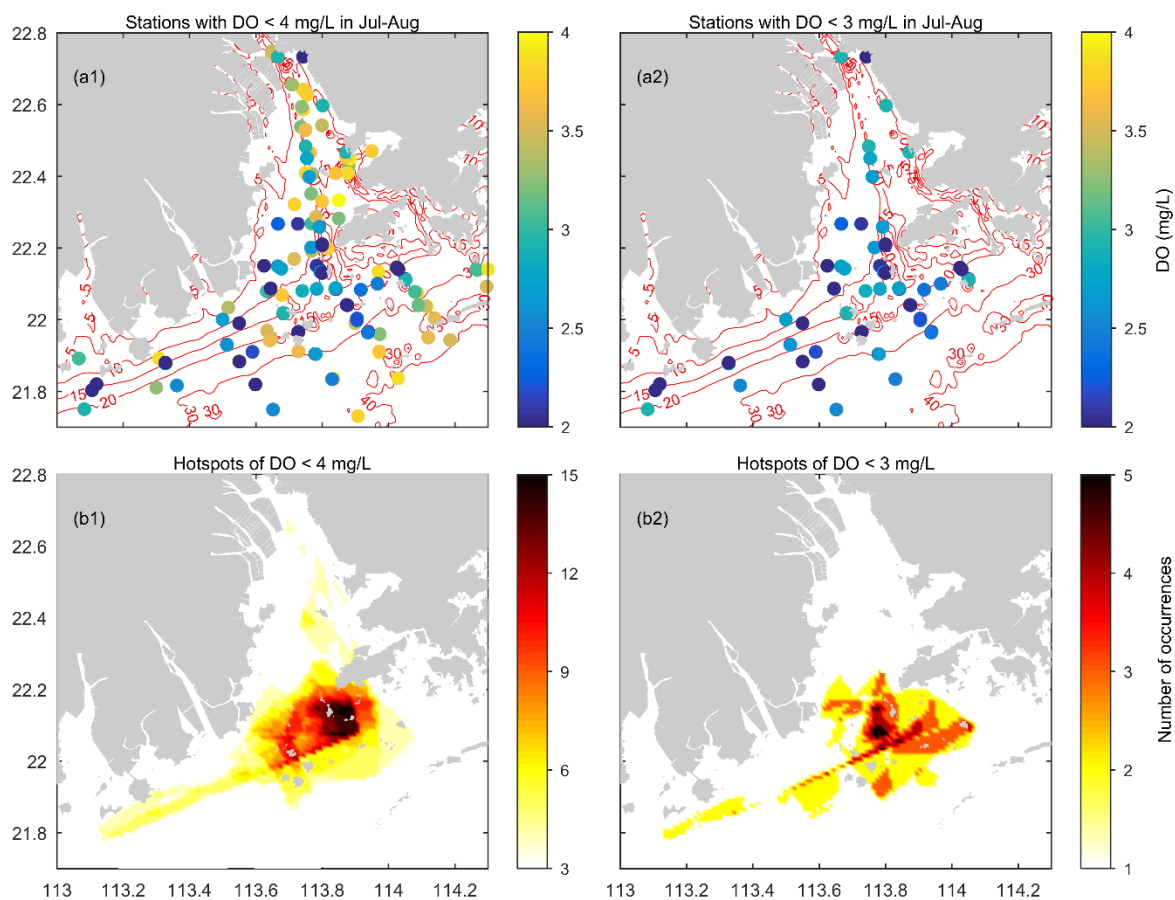
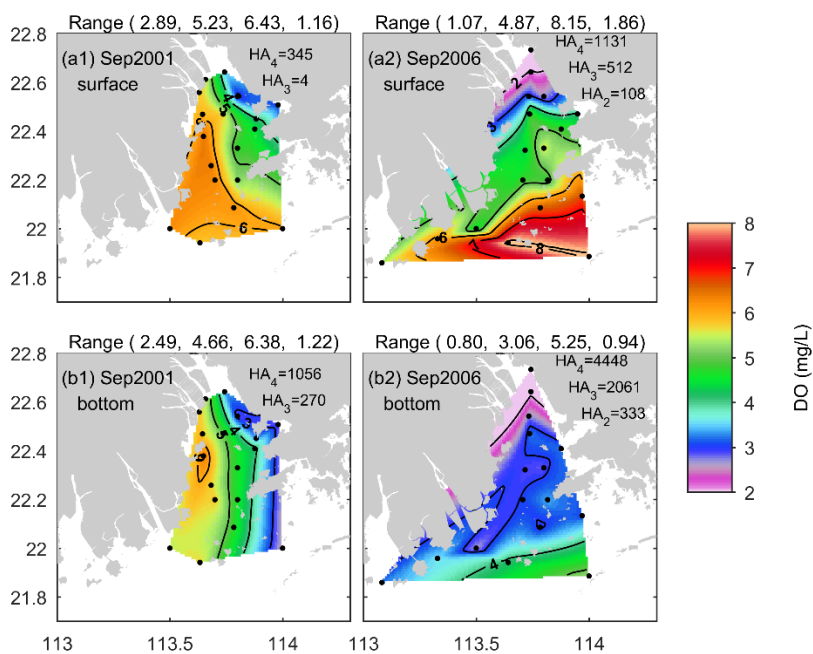


Figure 7. (a) The sites where low-oxygen conditions have been observed in the summer of the PRE and the corresponding lowest DO values measured (based on the data compiled from 1976 to 2017). (b) Maps showing the incidence of low-oxygen conditions at the bottom of the PRE in summer. Note that the darker color delineates higher occurrence of low-oxygen events.



635

Figure 8. DO distributions in the (a) surface and (b) bottom waters of the PRE for the early autumn (September) of 2001 (left panels) and 2006 (right panels).

640

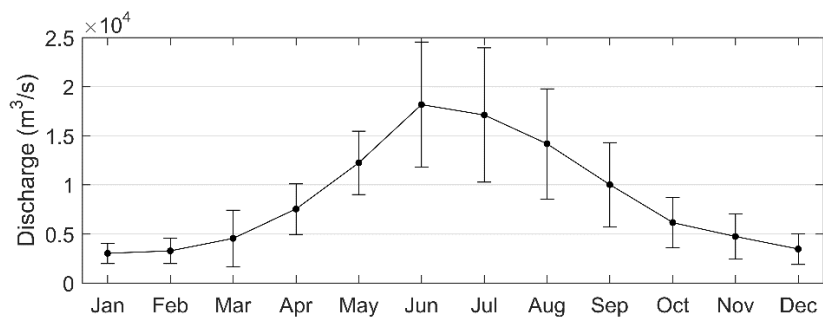


Figure 9. Monthly means and standard deviations of the Pearl River discharges calculated over 1979-2015.

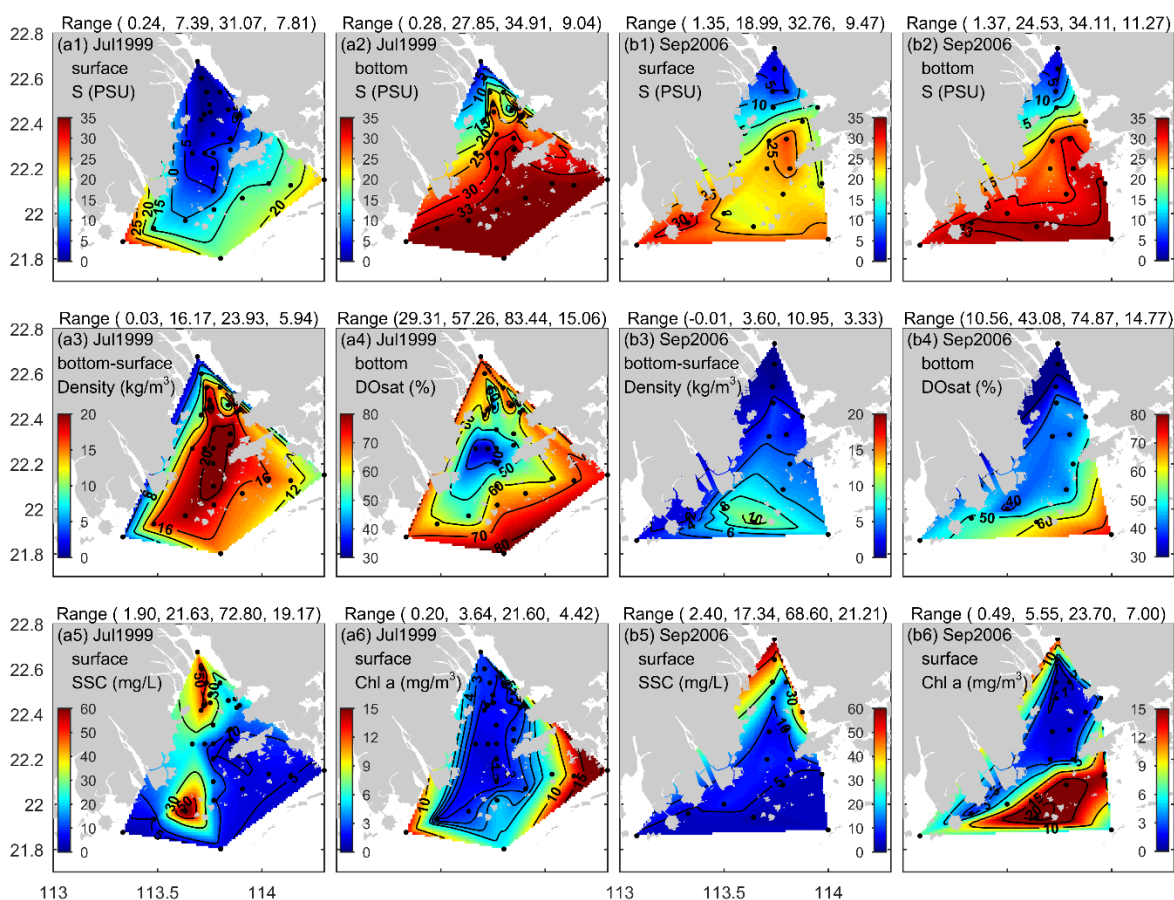


Figure 10. Comparison of water quality metrics observed in the PRE between (a) July 1999 (summer) and (b) 650 September 2006 (early autumn): surface and bottom salinity (top panels); vertical density difference and bottom DO saturation (DO_s) (middle panels); surface suspended sediment concentrations (SSC) and chlorophyll (chl) *a* contents (bottom panels). Note that the numbers in brackets in the titles are the minimum, mean, maximum, and standard deviation values of the associated water quality metrics in sequence.



655

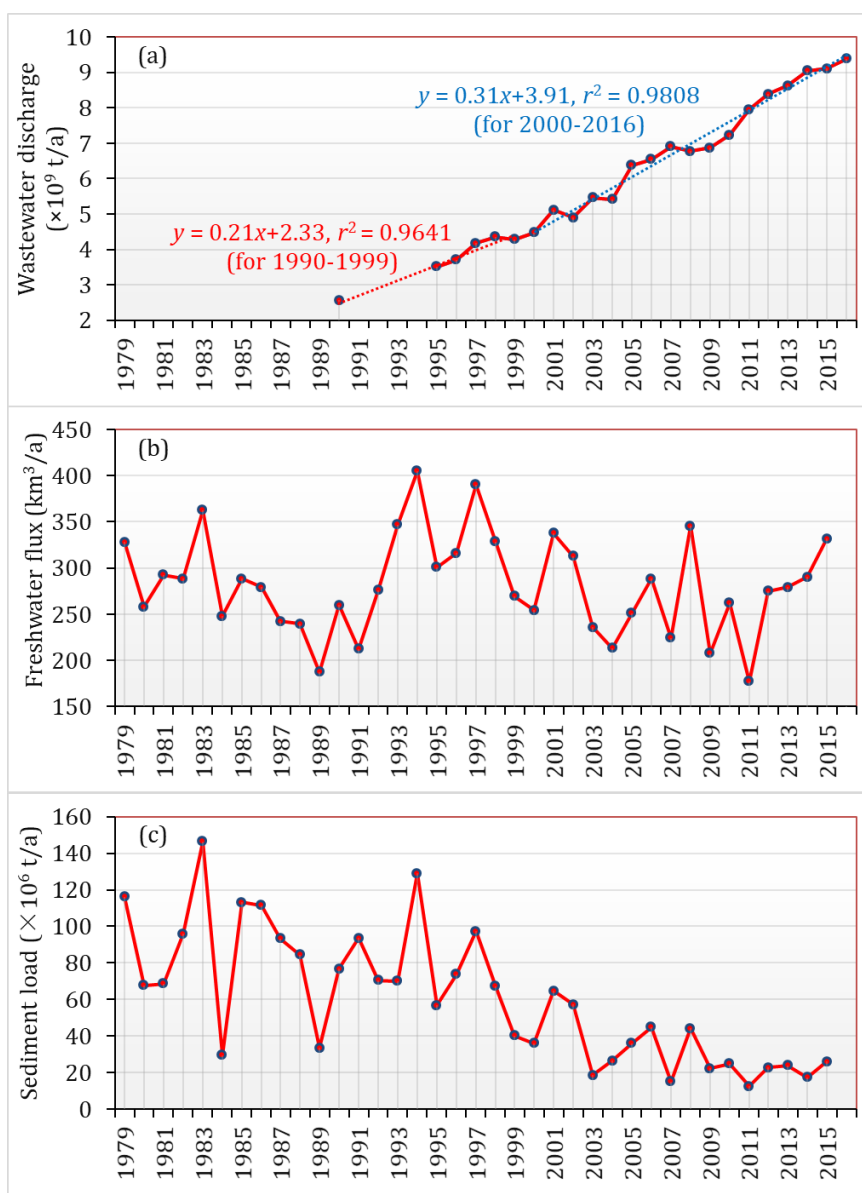


Figure 11. (a) Annual wastewater discharge in Guangdong Province during 1990-2016. The data before 1998 were taken from Li et al. (2020), and the remaining data were obtained from the Environmental Statistics Bulletin published by the Department of Ecology and Environmental of Guangdong Province (<http://gdee.gd.gov.cn/tjxx3187/index.html>).

660 (b) Freshwater discharge and (c) sediment load of the Pearl River from 1979 to 2015, adopted from Wu et al. (2020).